processes

MDPI

Article

Enhancing the Quality and Sustainability of Laser Cutting Processes in Laser-Assisted Manufacturing Using a Box–Behnken Design

Omid Mehrabi [1,*], Zeinab Malekshahi Beiranvand [2], Fakhir A. Rasoul [3] and Mahmoud Moradi [4,*]

[1] Department of Mechanical Engineering, Esfarayen University of Technology, Esfarayen 96619-98195, Iran
[2] Department of Materials, Faculty of Engineering, Arak University, Arak 38481-77584, Iran; z-malekshahi@araku.ac.ir
[3] Department of Air-Conditioning and Refrigeration Technical Engineering, College of Technical Engineering, Al-Kitab University, Kirkuk 36001, Iraq
[4] Faculty of Arts, Science and Technology, University of Northampton, Northampton NN1 5PH, UK
* Correspondence: omidmehrabi@esfarayen.ac.ir (O.M.); mahmoud.moradi@northampton.ac.uk (M.M.)

Abstract: This study aims to examine and optimize CO_2 laser cutting parameters—namely, laser power, cutting speed, and focal plane position—when applied to polypropylene material using an experimental methodology. This research aims to improve cutting quality, increase cutting speed, and reduce waste while adhering to sustainability objectives. To achieve these goals, a comprehensive experimental approach was employed, incorporating the Box–Behnken Design (BBD) based on the response surface methodology (RSM) to optimize the laser cutting process by evaluating the relationships between input parameters and output responses. Data were collected through a series of controlled experiments in which laser power (ranging from 30 to 60 W), cutting speed (ranging from 30 to 60 mm/s), and focal plane position (set at −3, 0, and +3 mm) were systematically varied. The responses, quantified regarding cut quality, include kerf width and the heat-affected zone (HAZ). Additionally, RSM was used to optimize the laser cutting process to improve kerf quality. The results indicated that cutting speed has an inverse effect on kerf width and HAZ, while laser power has a direct effect. Furthermore, the focal plane position was found to have the least impact on the output responses. The maximum kerf width and HAZ were observed at a minimum cutting speed of 30 mm/s and a maximum laser power of 60 W.

Keywords: laser material processing; optimization; CO_2 laser cutting; polypropylene; response surface methodology; Box–Behnken design; kerf width; heat-affected zone

check for updates

Academic Editor: Antaryami Mohanta

Received: 25 March 2025
Revised: 13 April 2025
Accepted: 21 April 2025
Published: 23 April 2025

Citation: Mehrabi, O.; Malekshahi Beiranvand, Z.; Rasoul, F.A.; Moradi, M. Enhancing the Quality and Sustainability of Laser Cutting Processes in Laser-Assisted Manufacturing Using a Box–Behnken Design. *Processes* **2025**, *13*, 1279. https://doi.org/10.3390/pr13051279

Copyright: © 2025 by the authors. Licensee MDPI, Basel, Switzerland. This article is an open access article distributed under the terms and conditions of the Creative Commons Attribution (CC BY) license (https://creativecommons.org/licenses/by/4.0/).

1. Introduction

Laser material processing (LMP) refers to a group of manufacturing techniques that utilize lasers for various processes such as laser milling [1], laser texturing [2], laser additive manufacturing [3,4], laser surface treatment [5], and laser cutting [6,7]. Laser cutting is widely used in the manufacturing industry for both metallic and non-metallic materials due to its superior precision, cut quality, and minimal waste compared to conventional cutting methods. A key advantage is its ability to shape, trim, and smooth components without requiring disassembly [8–10]. Despite the high quality typically associated with laser cutting, material failure may occasionally occur. This issue is primarily attributed to an insufficient understanding of the optimal input parameters that influence thermal damage, cutting quality, and the mechanical properties of the material. Carbon dioxide (CO_2) laser-cutting

machines are widely utilized due to their versatility and cost-effectiveness, supporting various applications such as marking, cutting, and engraving of plastic materials. The quality of laser cutting is primarily influenced by parameters like laser power (P), cutting speed (S), laser focal plane position (FPP), and the use of assisted gas. Moreover, factors such as the heat-affected zone (HAZ), surface roughness, and kerf width significantly contribute to the overall cutting quality [11–13]. For optimal performance, these parameters must be carefully balanced.

Polypropylene is a highly favored polymer in the manufacturing industry, particularly in the automobile sector, due to its excellent chemical resistance, lightweight nature, and superior thermal and mechanical properties [14,15]. Der et al. [16] studied the laser cutting of polyethylene and polyvinyl chloride using a CO_2 laser machine. The results indicated that the optimal cutting performance for polypropylene was achieved at a laser power of 90 W and a cutting speed of 15 mm/s. Choudhury and Shirley [17] investigated the effects of gas pressure, cutting speed, and laser power on the heat-affected zone (HAZ) and surface roughness of PP, polycarbonate (PC), and polymethyl methacrylate (PMMA) sheets using a central composite design (CCD). Their results demonstrated that PMMA exhibited the smallest HAZ, followed by PC, with PP showing the largest HAZ. In a separate study, Deepa et al. [18] examined the impacts of laser power and cutting speed on the hardness, maximum flexural stress, and ultimate tensile strength (UTS) of PP sheets. They employed a Grey Relational Analysis (GRA) to optimize multiple process parameters. The impact of nanosecond laser parameters, including repetition rate, cutting speed, and repetition time, on the kerf width and HAZ of PP sheets was studied by Wu et al. [19]. The smallest kerf width of 21.26 μm and HAZ of 16.92 μm were achieved with a repetition rate of 100 kHz, a cutting speed of 250 mm/s, and repeat times of 4.

Several studies have examined the cut quality of different polymers using CO_2 laser cutters [20–22]. Sabri et al. [23] evaluated the impacts of laser power, sheet thickness (t), and cutting speed on the kerf geometry dimensions of 3D-printed Polyethylene-Terephthalate-Glycol (PET-G) sheets. The effect of the laser cutting parameters on the top and bottom kerf width, the ratio of the top kerf to bottom kerf, and the HAZ were evaluated by using an analysis of variance (ANOVA). The results show that increases in the S and decreases in the P reduced the top and bottom kerf width and HAZ. Basar and Der et al. [24] used the integrating fuzzy analytic hierarchy process (AHP) and multi-criteria decision-making (MCDM) approaches to optimize focal length, laser power, and cutting speed, aiming to enhance cutting the kerf quality and surface roughness of polyethylene sheets. The results showed that the optimal parameters are a cutting speed of 12 mm/s, a power of 90 w, and a focal length of 8 mm. Aydın and Uğur [25] examined the effects of the focal plane, cutting speed, and laser power on the cutting kerf geometry dimensions and surface roughness PMMA sheets. The investigation employed an artificial neural network (ANN) and adaptive neuro-fuzzy inference system (ANFIS) to assess how cutting processing parameters influence the HAZ, kerf width at the cutting edge, and surface roughness. An experimental investigation explored the effect of two laser cutting parameters (cutting speed and laser power) on the cutting kerf quality of PLA sheets using a full factorial design [26]. Kechagiasa et al. [27] conducted a study that examined the influence of cutting speed, laser power, and stand-off distance (SoD) on the cutting kerf quality of PETG sheets by using the full factorial design method.

Based on a literature review, the main effects and interactions of cutting speed, laser power, and focal plane position on the cutting kerf quality of polypropylene sheets are less studied. Therefore, this research employs a scientific methodology—response surface methodology (RSM) and design of experiments (DOE)—to investigate the influence of laser cutting process parameters on the kerf width and heat-affected zone (HAZ) of PP sheets.

The results are analyzed and interpreted using a statistical analysis of variance (ANOVA). Finally, the Box–Behnken Design (BBD), based on RSM, was utilized to optimize the laser cutting parameters using Design-Expert software (State-Ease, version 12).

2. Experimental Methodology

2.1. Box–Behnken Design

Response surface methodology (RSM) is a set of mathematical and statistical techniques employed to model and analyze problems where the desired outcome is influenced by multiple input factors [28]. The primary objective is to optimize the efficiency of the process or reaction. This methodology generates a regression equation (Equation (1)) that accurately characterizes the relationship between the input variables (χ) and the response variable (y). The equation is expressed as follows: y denotes the predicted response, χ signifies the independent variables, β represents the regression coefficients, β_{ii} denotes the quadratic coefficients, β_{ij} represents the interaction coefficients, and ε accounts for the observed error [29,30].

$$y = \beta_0 + \sum_{i=1}^{k} \beta_i x_i + \sum_{i=1}^{k} \beta_{ii} x_i^2 + \sum_i \sum_j \beta_{ij} x_i x_j + \varepsilon \quad (1)$$

This study focuses on determining the impact of input parameters and identifying the optimal values for the CO_2 laser cutting of polypropylene. An RSM with the Box–Behnken design (BBD) is used to systematically plan the experiments using Design Expert 12 software (State-Ease, version 12, Minneapolis, MN, USA). The BBD is an RSM used to optimize processes by evaluating the relationships between input parameters and output responses [31,32]. Figure 1 shows the cubic design space constructed by the design matrix derived from the BBD. The experiment was designed by identifying key input parameters; analyzing previous studies to determine the most influential factors; and selecting the laser power (at three levels: 30, 45, and 60 W), cutting speed (at three levels: 30, 45, and 60 mm/s), and focal plane position (at three levels: −3, 0, and +3 mm) as the input parameters. Table 1 presents the details of the independent parameters and the corresponding levels of each parameter. Based on the BBD, the experimental design and corresponding results are listed in Table 2.

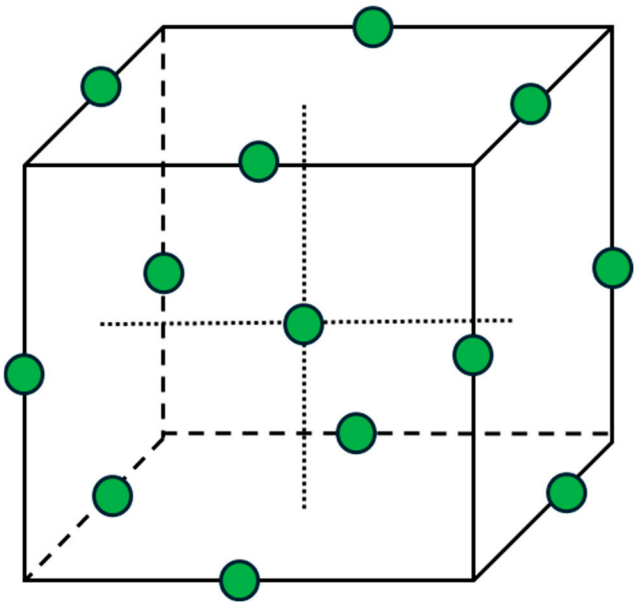


Figure 1. Schematic diagram of experimental design of three-parameter Box–Behnken design.

Table 1. Laser cutting parameters and corresponding levels of each parameter.

Variables	Notation	Unit	−1	0	+1
Laser power	P	w	30	45	60
Cutting speed	S	mm/s	30	45	60
Focal plane position	FPP	mm	−3	0	3

Table 2. Experimental design and results.

NO	Input Variables						Output Variables	
	Coded Values			Actual Values			Kerf with (μm)	HAZ (μm)
	P (W)	*S* (mm/s)	*FPP* (mm)	*P* (W)	*S* (mm/s)	*FPP* (mm)		
#1	−1	−1	0	30	30	0	588.5	1335.3
#2	−1	0	1	30	45	+3	499.3	1287.8
#3	1	0	1	60	45	+3	651.8	1383.5
#4	0	0	0	45	45	0	604.3	1430.2
#5	0	−1	1	45	30	+3	535.3	1517.3
#6	0	−1	−1	45	30	−3	703.6	1522.3
#7	0	1	1	45	60	+3	485	1509.4
#8	0	0	0	45	45	0	595.7	1427.3
#9	0	1	−1	45	60	−3	466.9	1019.4
#10	1	0	−1	60	45	−3	607.9	1671.9
#11	−1	0	−1	30	45	−3	562.6	1264.8
#12	1	1	0	60	60	0	551.1	1313.7
#13	0	0	0	45	45	0	595.7	1385.6
#14	−1	1	0	30	60	0	414.4	827.3
#15	1	−1	0	60	30	0	585.6	1654.7

2.2. Experimental Work

This study used a polypropylene sheet with dimensions of 50 cm × 60 cm × 0.7 mm. Polypropylene, a widely utilized thermoplastic material in various industries, presents unique challenges and opportunities in laser cutting processes. Table 3 presents the properties of the PP sheet. The laser cutting experiments were performed using a continuous-wave (CW) CO_2 laser cutting machine operating at a wavelength of 1060 nm. The laser beam had a Gaussian profile with a spot size of 0.2 mm at the focal plane. A total of 15 distinct cuts were made, each corresponding to a unique combination of input parameters, as outlined in Table 2. All laser cutting experiments were conducted at a room temperature of 25 ± 1 °C. Figure 2 shows the schematic of the CO_2 laser cutting process used in this study.

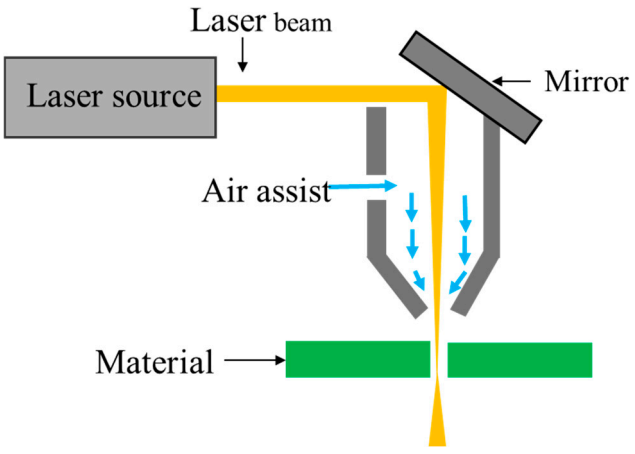


Figure 2. Schematic of laser cutting process.

Table 3. Properties of the PP sheet used in this study [18].

Property	Unite	Value
Density	g/cm^3	0.91
Melting point	°C	160
Modulus of Elasticity	GPa	0.9–1.1
Electrical Resistivity	Ω/cm	10^{16}–10^{18}
Thermal Coefficient	---	72–90

After the laser cutting process, an optical microscope was employed to measure the kerf width and heat-affected zone (HAZ) to assess the cutting quality. Based on Figure 3, the kerf width and the heat-affected zone (HAZ) of the cutting kerf were measured using ImageJ software (version 1.54p).

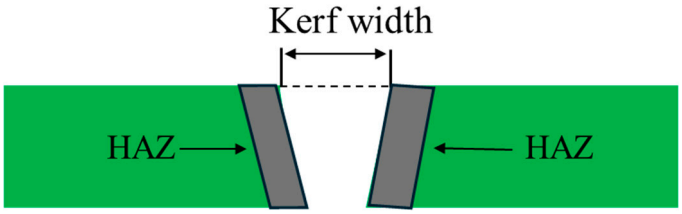


Figure 3. Schematic of cutting kerf geometry.

3. Results and Discussion

The responses, including kerf width, depth of the cut, and HAZ, were analyzed by generating an ANOVA table. An ANOVA table presents the results of an ANOVA test, in which the probability connected to the F-statistic is known as the *p*-value.

3.1. Analysis of the Width of the Kerf

The kerf width in laser cutting refers to the width of the cut or groove created by the laser beam as it removes material during the cutting process. An analysis of variance (ANOVA) table (Table 4) was generated using Expert 12 software to determine the significant and insignificant parameters affecting kerf width statistically. According to Table 4, the *p*-values of the main laser cutting parameters—laser power (P), cutting speed (S), and focal plane position (FPP)—along with their interaction terms and the quadratic terms of P (A^2) and S (B^2), are all less than 0.05. This indicates that these parameters have a significant effect on kerf width. The F-values for P, S, and FPP are 371.40, 179.06, and 22.65, respectively, suggesting that cutting speed has the most significant effect on kerf width, followed by laser power and focal plane position. The final regression equation for the kerf width model is presented in Equation (2) (in terms of actual factors).

$$\begin{aligned}(Kerf\ width)^{-1.98} &= +\left(5.33999\times10^{-6}\right)+\left(8.58352\times10^{-9}\times P\right)-\left(8.58352\times10^{-9}\times S\right)\\ &+\left(9.22082\times10^{-7}\times FPP\right)-\left(3.1840\times P\times S\right)-\ \left(7.51538\times10^{-9}\times P\times FPP\right)\\ &-\ \left(1.12712\times10^{-8}\times S\times FPP\right)+\ \left(1.01751\times10^{-9}\times P^2\right)+\left(3.65871\times10^{-9}\times S^2\right)\\ &+\left(7.74143\times10^{-9}\times FPP^2\right)\end{aligned} \quad (2)$$

Kerf width is a critical parameter for evaluating the performance of the laser cutting process, as it directly affects the quality of the cut. The main effect plot of kerf width (Figure 4) illustrates that the cut width increases with rising laser power and decreasing cutting speed. It has been observed that kerf width is inversely proportional to cutting speed and directly proportional to laser power. An increase in laser power raises the temperature in the cutting zone, generating more molten metal and resulting in a wider

kerf, especially at lower cutting speeds. These findings are consistent with the research conducted by Ming [33] and Yilbas [34], who reported that an increase in laser power (P) and a decrease in cutting speed (S) resulted in a wider kerf width. Ultimately, it is evident that within the range of the focal plane position examined in this study, FPP has a negligible effect on the kerf width. In contrast, laser speed and power exhibit a more significant influence.

Table 4. ANOVA results for kerf width.

Source	Sum of Squares	df	Mean Square	F-Value	*p*-Value
Model	1.686×10^{-11}	9	1.873×10^{-12}	100.20	<0.0001
A—Laser power	3.347×10^{-12}	1	3.347×10^{-12}	179.06	<0.0001
B—Cutting speed	6.942×10^{-12}	1	6.942×10^{-12}	371.40	<0.0001
C—Focal plane position	4.234×10^{-13}	1	4.234×10^{-13}	22.65	0.0051
AB	2.053×10^{-12}	1	2.053×10^{-12}	109.83	0.0001
AC	4.575×10^{-13}	1	4.575×10^{-13}	24.48	0.0043
BC	1.029×10^{-12}	1	1.029×10^{-12}	55.05	0.0007
A^2	1.935×10^{-13}	1	1.935×10^{-13}	10.35	0.0235
B^2	2.502×10^{-12}	1	2.502×10^{-12}	133.87	<0.0001
C^2	1.792×10^{-14}	1	1.792×10^{-14}	0.9589	0.3724
Residual	9.345×10^{-14}	5	1.869×10^{-14}		
Lack of Fit	8.806×10^{-14}	3	2.935×10^{-14}	10.88	0.0853
Pure Error	5.395×10^{-15}	2	2.697×10^{-15}		
Cor Total	1.695×10^{-11}	14			
$R^2 = 0.99$			Adjusted $R^2 = 0.98$		

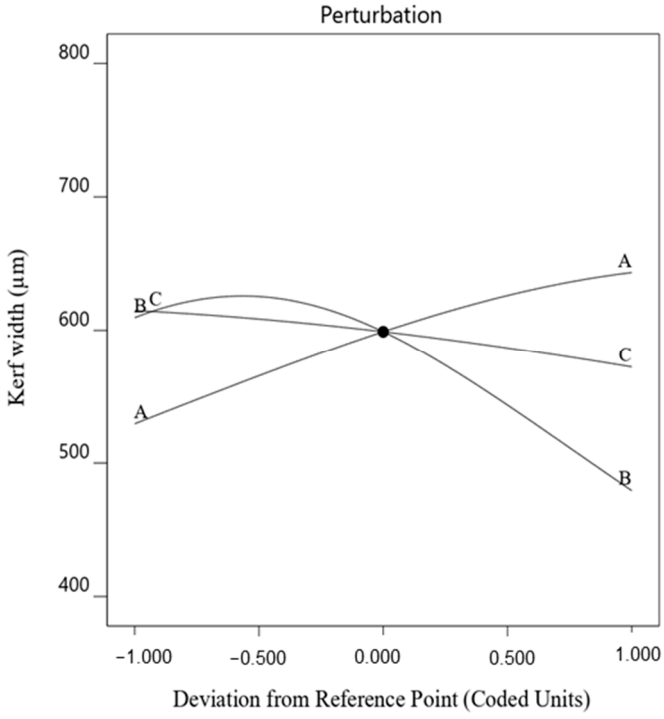
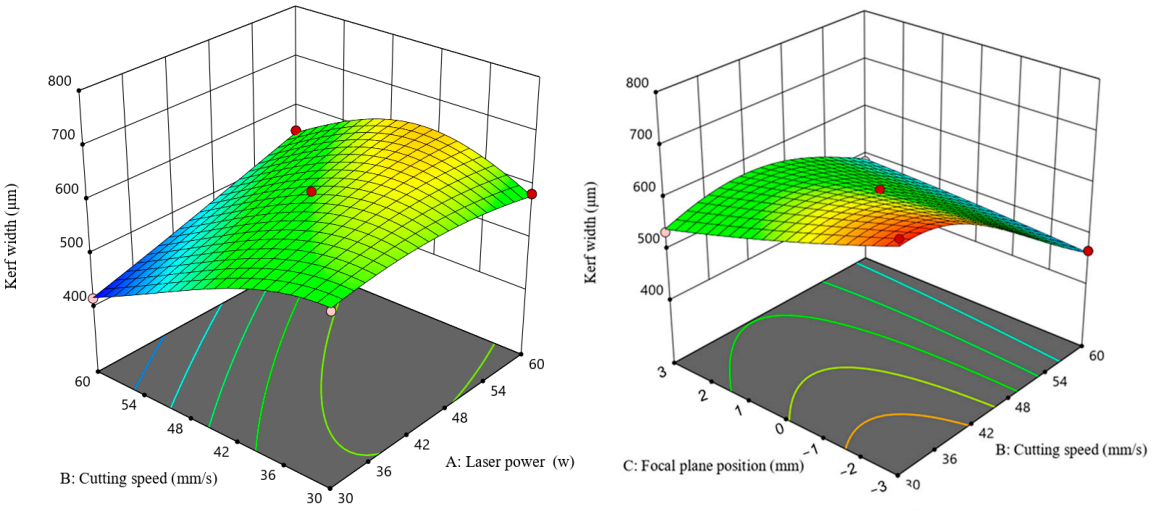


Figure 4. Main effect plot for kerf width (A = laser power, B = cutting speed, C = focal plane position).

The surface plot is a three-dimensional graphical representation used to evaluate the response of the kerf width concerning cutting speed, laser power, and focal plane position. In this plot, kerf width is depicted along the *z*-axis, while cutting speed, laser power, and focal plane position are represented on the *x*- and *y*-axes. Figure 5 provides a detailed visualization of how these parameters influence the kerf width. Figure 5a,b show that FPP only slightly affects kerf width, unlike the significant impact of laser power and

cutting speed on kerf width. Kerf width can be decreased by minimizing laser power and maximizing cutting speed. According to Figure 5a, the lowest kerf width is observed at 60 mm/s cutting speed and 30 w power.



(**a**) (**b**)

Figure 5. Three-dimensional surface plot for response kerf width, (**a**) effect of interaction cutting speed and laser power on kerf width, (**b**) effect of interaction cutting speed and focal position on kerf width.

3.2. Analysis of Heat-Affected Zone (HAZ)

Table 5 presents the ANOVA table for the heat-affected zone (HAZ), generated using response surface methodology (RSM). The ANOVA results show that cutting speed (S, represented by term B) and laser power (P, represented by term A) are significant factors influencing the HAZ in the CO_2 laser cutting of polypropylene. The regression equation derived from the primary data analysis is shown in Equation (3).

$$(heat\ affected\ zone)^{2.74} = +(3.98037 \times 10^8) + (8.16353 \times 10^6 \times P) - (7.78498 \times 10^6 \times S) + (3.09578 \times 10^6 \times FPP) \quad (3)$$

Table 5. ANOVA results for HAZ.

Source	Sum of Squares	df	Mean Square	F-Value	*p*-Value
Model	2.297×10^{17}	3	7.658×10^{16}	7.34	0.0057
A—Laser power	1.200×10^{17}	1	1.200×10^{17}	11.50	0.0060
B—Cutting speed	1.091×10^{17}	1	1.091×10^{17}	10.46	0.0080
C—Focal plane position	6.900×10^{14}	1	6.900×10^{14}	0.0661	0.8018
Residual	1.148×10^{17}	11	1.043×10^{16}		
Lack of Fit	1.139×10^{17}	9	1.266×10^{16}	29.91	0.0328
Pure Error	8.463×10^{14}	2	4.232×10^{14}		
Cor Total	3.445×10^{17}	14			
$R^2 = 0.66$			Adjusted $R^2 = 0.57$		

Figure 6 presents the main effect plot for HAZ, illustrating the impact of laser power, cutting speed, and focal plane position. HAZ increases with decreasing laser power and increasing cutting speed, and increasing the laser power results in a higher energy input, which raises the temperature of the material over a broader region. This extended heat exposure causes the thermal gradient to spread farther from the cut, enlarging the

HAZ [35,36]. Simultaneously, decreasing the cutting speed means the laser remains in contact with a given point on the material for longer. This prolonged interaction allows more heat to diffuse into the surrounding areas, further expanding the HAZ [17,36]. The results illustrated in Figure 6 indicate that variations in the FPP exert a negligible influence on the heat-affected zone HAZ.

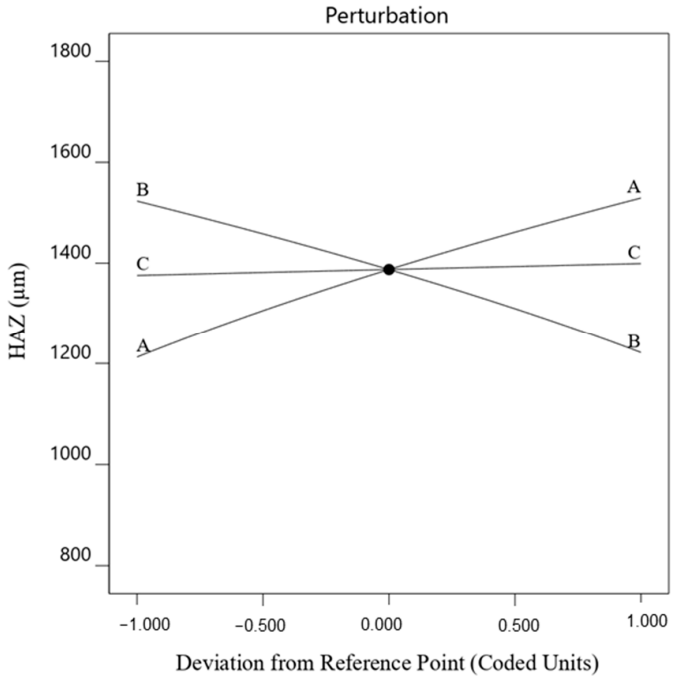
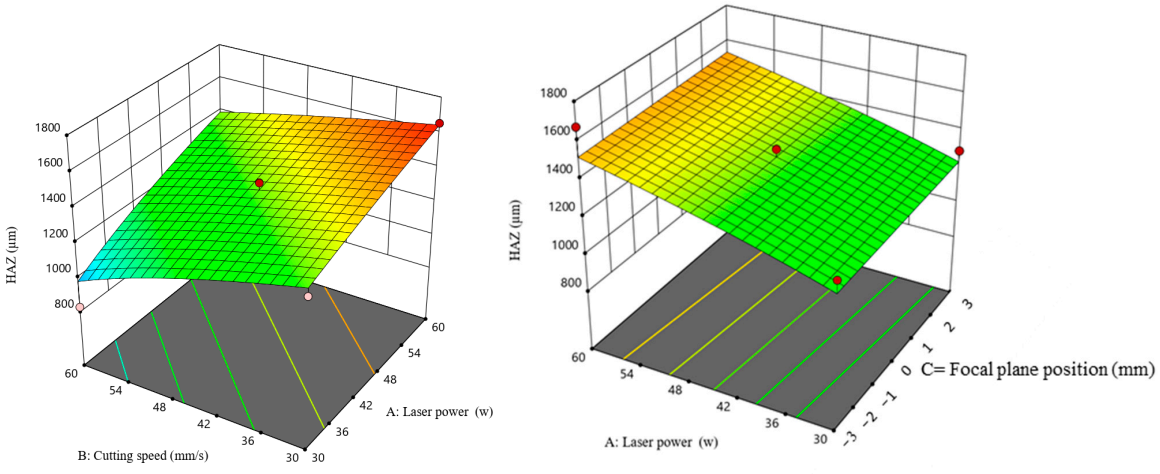


Figure 6. Main effect plot for HAZ (A = laser power, B = cutting speed, C = focal plane position).

Figure 7a shows the variation in the HAZ based on the combined impact of S (30 to 60 mm/s) and P (30 to 60 W), while Figure 7b shows the variation in HAZ based on the combined impact of FPP (30 to 60 mm) and P (30 to 60 W). The surface plot reveals that the HAZ reaches its minimum at the highest cutting speed (60 mm/s) and maximum laser power (60 W). Conversely, the maximum HAZ occurs at the lowest cutting speed (30 mm/s) and maximum laser power (60 W).



(**a**) (**b**)

Figure 7. Three-dimensional surface plot for response HAZ, (**a**) effect of interaction cutting speed and laser power on HAZ, (**b**) effect of interaction laser power and focal plane position HAZ.

4. Optimization

In general, various methods and algorithms can be used for numerical optimization [37–39], with response surface methodology (RSM) being one of the most widely used techniques for optimization [40]. The main objective of this study is to achieve precise and smooth cutting of polypropylene materials using a CO_2 laser cutting machine. To accomplish this, the goal is to minimize the heat-affected zone (HAZ) and kerf width. These objectives serve as the foundation for the optimization process, with detailed information provided in Table 6. Table 6 sets specific goals for each response, with minimum values defined. The targets for optimization are based on these goals. To achieve better quality cuts, each response is assigned equal weight and importance, with a weightage of 1 for each response. The optimal solution is the set of values for the decision variables that yields the best possible outcome according to the objective function while satisfying all constraints. The solution, in terms of actual values, generated using Design Expert 12 software for the response surface design, is presented in Table 7. Figure 8 shows the desirability graph representing the impact of laser cutting and laser power on output responses, predicting the actual responses for kerf width and heat-affected zone (HAZ) at the desired levels of input parameters. The solution obtained from Design Expert 12 software for optimal cutting quality suggests the following values: laser power at 30 watts, cutting speed at 60 mm/s, and focal plane at −3 mm. With this combination, the heat-affected zone (HAZ) will be 1001.314 µm, and the cut width will be 415.721 µm. The desirability of the solution is 0.935.

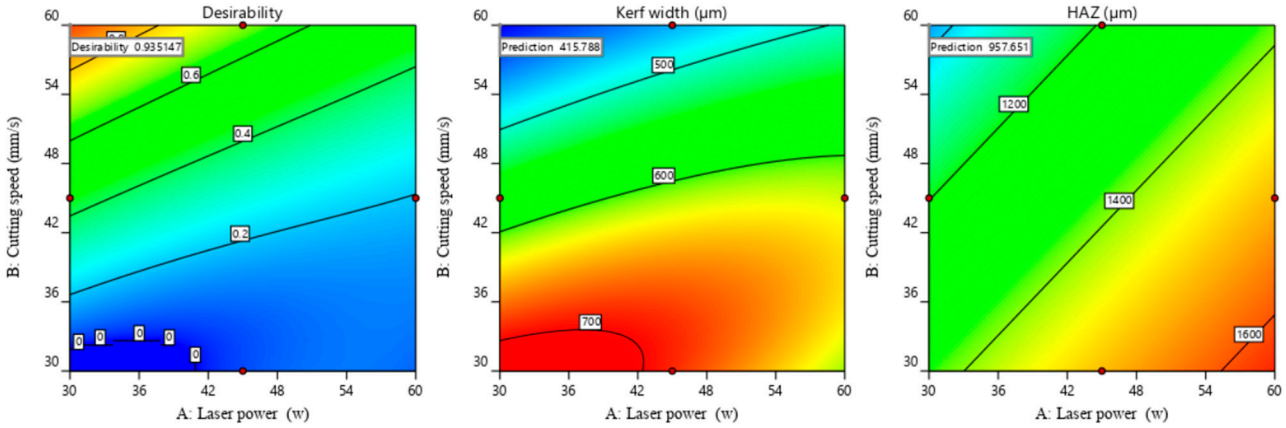


Figure 8. The desirability graph representing the effect of laser cutting and laser power on output responses, predicting the actual responses for kerf width and heat-affected zone (HAZ) at the desired levels of input parameters.

Table 6. Optimization criteria.

Parameter/Response			Goal	Lower	Upper	Importance
Parameter		Laser power	In range	30	60	-
		Cutting speed	In range	30	60	-
		Focal plane position	In range	−3	+3	-
Response	Criteria Set 1	Kerf width	Minimize	414.388	703.597	3
		Heat-Affected Zone	Minimize	827.338	1671.94	3
	Criteria Set 2	Kerf width	Minimize	414.388	703.597	2
		Heat-Affected Zone	Minimize	827.338	1671.94	5
	Criteria Set 3	Kerf width	Minimize	414.388	703.597	5
		Heat-Affected Zone	Minimize	827.338	1671.94	2

Table 7. Optimization result.

Solution	Laser Power	Cutting Speed	Focal Plane Position	Kerf Width	HAZ	Desirability
1	30.000	60.000	−3.000	415.721	1001.314	0.935
2	30.000	60.000	−2.999	415.720	1001.294	0.912
3	30.000	60.000	−3.000	415.721	1001.293	0.958

5. Conclusions

This study investigates the CO_2 laser cutting technology for polypropylene materials and aims to optimize input parameters using response surface methodology (RSM) to enhance cut quality, cutting speed, and overall performance. The key findings include the following:

- The experiments conducted using the response surface methodology (RSM) show that cutting speed and laser power have a significant influence on both kerf width and HAZ. In contrast, within the range of focal plane position (FPP) examined in this study, FPP exhibits a negligible effect on kerf width and HAZ.
- The findings show that a decrease in cutting speed and an increase in laser power increase both kerf width and HAZ.
- The lowest kerf width (414.388 μm) and HAZ (827.338 μm) are observed at a cutting speed of 60 mm/s and a laser power of 30 W.
- The results indicated that the optimal parameter settings for achieving the minimum kerf width and HAZ are a cutting speed of 60 mm/s, a laser power of 30 W, and a focal plane position of −3 mm.

Author Contributions: Methodology, Z.M.B. and M.M.; Software, O.M.; Validation, F.A.R.; Writing—original draft, O.M. and Z.M.B.; Writing—review and editing, F.A.R. and M.M.; Visualization, O.M., Z.M.B. and M.M.; Supervision, F.A.R. and M.M. All authors contributed equally to this work. All authors have read and agreed to the published version of the manuscript.

Funding: This research received no external funding.

Data Availability Statement: The original contributions presented in this study are included in this article; further inquiries can be directed to the corresponding author.

Conflicts of Interest: The authors declare no conflicts of interest.

References

1. Chi, Y.; Dong, Z.; Cui, M.; Shan, C.; Xiong, Y.; Zhang, D.; Luo, M. Comparative study on machinability and surface integrity of γ-TiAl alloy in laser assisted milling. *J. Mater. Res. Technol.* **2024**, *33*, 3743–3755. [CrossRef]
2. Zhou, Y.; Zhang, Q.; Li, X.; Wang, Y.; Guan, Y. Mechanical performance of laser-textured metallic surface. *J. Mater. Res. Technol.* **2024**, *33*, 6084–6089. [CrossRef]
3. Luo, W.; Yuan, X.; Zhang, Z.; Cheng, C.; Liu, H.; Qiu, H.; Cheng, X. Effect of volumetric energy density on the mechanical properties and corrosion resistance of laser-additive-manufactured $AlCoCrFeNi_{2.1}$ high-entropy alloys. *J. Alloys Compd.* **2025**, *1010*, 178032. [CrossRef]
4. Mehrabi, O.; Seyedkashi, S.; Moradi, M. Effect of the Laser Power on the Geometrical Features of 316L Stainless Steel Additively Manufactured by Direct Laser Metal Deposition (DLMD). *Lasers Eng.* **2023**, *56*, 127–141.
5. Cui, M.; Shi, G.; Deng, L.; Guo, H.; Xiong, S.; Tan, L.; Yao, C.; Zhang, D.; Deguchi, Y. Microstructure classification of steel samples with different heat-treatment processes based on laser-induced breakdown spectroscopy (LIBS). *J. Anal. At. Spectrom.* **2024**, *39*, 1361–1374. [CrossRef]
6. Cui, M.; Shilei, X.; Nan, Y.; Yuanbin, W.; Zhenzhen, W.; Ming, L.; Changfeng, Y. Deguchi Applications of laser-induced breakdown spectroscopy in industrial measurement and monitoring: Multi-technology combination. *Appl. Spectrosc. Rev.* **2025**, *60*, 243–291. [CrossRef]

7. Moradi, M.; Mehrabi, O.; Azdast, T.; Benyounis, K.Y. Enhancement of low power CO_2 laser cutting process for injection molded polycarbonate. *Opt. Laser Technol.* **2017**, *96*, 208–218. [CrossRef]
8. Alsaadawy, M.; Dewidar, M.; Said, A.; Maher, I.; Shehabeldeen, T.A. A comprehensive review of studying the influence of laser cutting parameters on surface and kerf quality of metals. *Int. J. Adv. Manuf. Technol.* **2024**, *130*, 1039–1074. [CrossRef]
9. Naresh; Khatak, P. Laser cutting technique: A literature review. *Mater. Today Proc.* **2022**, *56*, 2484–2489. [CrossRef]
10. Moradi, M.; Mehrabi, O.; Azdast, T.; Benyounis, K.Y. Effect of the focal plane position on CO_2 laser beam cutting of injection molded polycarbonate sheets. *Second. Int. Semin. Photonics Opt. Its Appl.* **2016**, *10150*, 56–65.
11. Adin, M.Ş. Investigation of the Effects of Machining Parameters on Kerf Widths during Laser Beam Machining of Medium Carbon Steels. *J. Mater. Eng. Perform.* **2025**, *34*, 5304–5315. [CrossRef]
12. Patel, A.; Bhavsar, S.N. Experimental investigation to optimize laser cutting process parameters for difficult to cut die alloy steel using response surface methodology. *Mater. Today Proc.* **2021**, *43*, 28–35. [CrossRef]
13. Wang, J.; Sun, Z.; Gu, L.; Azimy, H. Investigating the effect of laser cutting parameters on the cut quality of Inconel 625 using Response Surface Method (RSM). *Infrared Phys. Technol.* **2021**, *118*, 103866. [CrossRef]
14. Agarwal, J.; Sahoo, S.; Mohanty, S.; Nayak, S.K. Progress of novel techniques for lightweight automobile applications through innovative eco-friendly composite materials: A review. *J. Thermoplast. Compos. Mater.* **2020**, *33*, 978–1013. [CrossRef]
15. Huang, P.; Su, Y.; Luo, H.; Lan, X.; Chong, Y.; Wu, F.; Zheng, W. Facile one-step method to manufacture polypropylene bead foams with outstanding thermal insulation and mechanical properties via supercritical CO_2 extrusion foaming. *J. CO2 Util.* **2022**, *64*, 102167. [CrossRef]
16. Der, O.; Ordu, M.; Basar, G. Optimization of cutting parameters in manufacturing of polymeric materials for flexible two-phase thermal management systems. *Mater. Test.* **2024**, *66*, 1700–1719. [CrossRef]
17. Choudhury, I.A.; Shirley, S. Laser cutting of polymeric materials: An experimental investigation. *Opt. Laser Technol.* **2010**, *42*, 503–508. [CrossRef]
18. Deepa, A.; Padmanabhan, K.; Kuppan, P. Analysis and optimization of machining parameters of laser cutting for polypropylene composite. In *IOP Conference Series: Materials Science and Engineering, Vellore, India, 2–3 May 2017*; IOP Publishing: Bristol, UK, 2017; Volume 263, p. 062043. [CrossRef]
19. Wu, C.; Rong, Y.; Li, M.; Zhang, G.; Huang, Y.; Zhang, T. High-quality cutting of polypropylene (PP) film by UV nanosecond laser based on thermal ablation. *Opt. Laser Technol.* **2022**, *147*, 107600. [CrossRef]
20. Singh, Y.; Singh, J.; Sharma, S.; Aggarwal, V.; Pruncu, C.I. Multi-objective Optimization of Kerf-taper and Surface-roughness Quality Characteristics for Cutting-operation On Coir and Carbon Fibre Reinforced Epoxy Hybrid Polymeric Composites During CO_2-Pulsed Laser-cutting Using RSM. *Lasers Manuf. Mater. Process.* **2021**, *8*, 157–182. [CrossRef]
21. Singh, Y.; Singh, J.; Sharma, S.; Sharma, A.; Chohan, J.S. Process parameter optimization in laser cutting of Coir fiber reinforced Epoxy composite—A review. *Mater. Today Proc.* **2022**, *48*, 1021–1027. [CrossRef]
22. Elsheikh, A.H.; Muthuramalingam, T.; Elaziz, M.A.; Ibrahim, A.M.M.; Showaib, E.A. Minimization of fume emissions in laser cutting of polyvinyl chloride sheets using genetic algorithm. *Int. J. Environ. Sci. Technol.* **2022**, *19*, 6331–6344. [CrossRef]
23. Sabri, H.; Mehrabi, O.; Khoran, M.; Moradi, M. Leveraging CO_2 laser cutting for enhancing fused deposition modeling (FDM) 3D printed PETG parts through postprocessing. *Proc. Inst. Mech. Eng. Part E J. Process Mech. Eng.* **2024**. [CrossRef]
24. Basar, G.; Der, O. Multi-objective optimization of process parameters for laser cutting polyethylene using fuzzy AHP-based MCDM methods. *Proc. Inst. Mech. Eng. Part E J. Process Mech. Eng.* **2025**. [CrossRef]
25. Aydın, K.; Uğur, L. Prediction of Kerf and Groove Widths in CO_2 Laser Cutting Process of PMMA Using Experimental and Machine Learning Methods. *Exp. Tech.* **2025**, 1–14. [CrossRef]
26. Kechagias, J.D.; Ninikas, K.; Petousis, M.; Vidakis, N.; Vaxevanidis, N. An investigation of surface quality characteristics of 3D printed PLA plates cut by CO_2 laser using experimental design. *Mater. Manuf. Process.* **2021**, *36*, 1544–1553. [CrossRef]
27. Kechagias, J.D.; Fountas, N.A.; Ninikas, K.; Petousis, M.; Vidakis, N.; Vaxevanidis, N. Surface characteristics investigation of 3D-printed PET-G plates during CO_2 laser cutting. *Mater. Manuf. Process.* **2022**, *37*, 1347–1357. [CrossRef]
28. Moradi, M.; Mehrabi, O.; Rasoul, F.A.; Mattie, A.A.; Schaber, F.; Khandan, R. Enhancing 3D Printing Copper-PLA Composite Fabrication via Fused Deposition Modeling through Statistical Process Parameter Study. *Micromachines* **2024**, *15*, 1082. [CrossRef] [PubMed]
29. Jensen, W.A. *Response Surface Methodology: Process and Product Optimization Using Designed Experiments*, 4th ed.; Taylor & Francis, Ed.; Wiley: Hoboken, NJ, USA, 2017.
30. Agha, H.M.; Abdulhameed, A.S.; Jawad, A.H.; Alothman, Z.A.; Wilson, L.D.; Algburi, S. Fabrication of glutaraldehyde crosslinked chitosan/algae biomaterial via hydrothermal process: Statistical optimization and adsorption mechanism for MV 2B dye removal. *Biomass Convers. Biorefinery* **2025**, *15*, 1105–1119. [CrossRef]
31. Khan, M.K.A.; Abdulhameed, A.S.; Alshahrani, H.; Algburi, S. Development of chitosan biopolymer by chemically modified orange peel for safranin O dye removal: A sustainable adsorbent and adsorption modeling using RSM-BBD. *Int. J. Biol. Macromol.* **2024**, *261*, 129964. [CrossRef]

32. Agha, H.M.; Abdulhameed, A.S.; Jawad, A.H.; Sidik, N.J.; Aazmi, S.; ALOthman, Z.A.; Wilson, L.D.; Algburi, S. Physicochemical fabrication of chitosan and algae with crosslinking glyoxal for cationic dye removal: Insight into optimization, kinetics, isotherms, and adsorption mechanism. *Int. J. Biol. Macromol.* **2023**, *253*, 127112. [CrossRef]
33. Li, M. Evaluation of the effect of process parameters on the cut quality in fiber laser cutting of duplex stainless steel using response surface method (RSM). *Infrared Phys. Technol.* **2021**, *118*, 103896. [CrossRef]
34. Rajesh, K.; Raju, V.V.M.K.; Rajesh, S.; Varma, N.S.K. Effect of process parameters on machinability characteristics of CO_2 laser process used for cutting SS-304 Stainless steels. *Mater. Today Proc.* **2019**, *18*, 2065–2072. [CrossRef]
35. Leone, C.; Mingione, E.; Genna, S. Laser cutting of CFRP by Quasi-Continuous Wave (QCW) fibre laser: Effect of process parameters and analysis of the HAZ index. *Compos. Part B Eng.* **2021**, *224*, 109146. [CrossRef]
36. Son, S.; Lee, D. The Effect of Laser Parameters on Cutting Metallic Materials. *Materials* **2020**, *13*, 4596. [CrossRef]
37. Tao, Z.; Li, W.; Guo, Z.; Chen, Y.; Song, L.; Li, J. Aerothermal optimization of a turbine rotor tip configuration based on free-form deformation approach. *Int. J. Heat Fluid Flow* **2024**, *110*, 109644. [CrossRef]
38. Long, X.; Lu, C.; Su, Y.; Dai, Y. Machine learning framework for predicting the low cycle fatigue life of lead-free solders. *Eng. Fail. Anal.* **2023**, *148*, 107228. [CrossRef]
39. Peng, X.; Chen, K.; Jia, W.; Li, K.; Huang, C.; Liu, X. Stacking sequence optimization of variable thickness composite laminated plate based on multi-peak stacking sequence table. *Compos. Struct.* **2025**, *356*, 118886. [CrossRef]
40. Guo, X.; Tian, D.; Li, C.; Li, X.; Li, W.; Cao, M.; Zhang, F.; Wang, B. Optimization for the Process Parameters of Nickel–Titanium Nitride Composites Fabricated via Jet Pulse Electrodeposition. *Nanomaterials* **2024**, *14*, 2034. [CrossRef]

Disclaimer/Publisher's Note: The statements, opinions and data contained in all publications are solely those of the individual author(s) and contributor(s) and not of MDPI and/or the editor(s). MDPI and/or the editor(s) disclaim responsibility for any injury to people or property resulting from any ideas, methods, instructions or products referred to in the content.